Simulation of fiber deposition on 3d printed molded fiber screen using multi-sphere discrete element method

K. Q. Le[1,2], J. W. Chew[1,3], M. F. Leyva-Mendivil[1,4], T. H. Thai[5], F. Duan[1,6,*]

[1]HP-NTU Digital Manufacturing Corporate Lab, Nanyang Technological University, 639798, Singapore

[2]Vietnam Japan University, Vietnam National University, Hanoi, Vietnam

[3]School of Chemistry, Chemical Engineering and Biotechnology, Nanyang Technological University, 639798, Singapore

[4]3D Lab, HP Labs, HP Inc., Palo Alto, California 94304, USA

[5]Asia East University of Technology, Vietnam

[6]School of Mechanical and Aerospace Engineering, Nanyang Technological University, 639798, Singapore

* Corresponding author. E-mail address: feiduan@ntu.edu.sg

Abstract

In line with the sustainable development goal, molded fiber products play important roles in reducing plastic-based packaging. To fabricate molded fiber products, besides using conventional meshing tools, 3D printing is employed to manufacture the molded fiber screen. 3D printing technique allows printing molded fiber screens with complex geometry, flexible in pore size and shape. The 3D printed molded fiber screens are in the process of investigation to improve the de-watering efficiency, fiber collection, mechanical strength, etc. In addition, the fiber distribution on the screen is also necessary to assess the quality of the screen. Besides using experimental methods to capture the fiber distribution on screen, simulation also offers using tools to assess the uniformity of the fiber. In this study, the multi-sphere model was employed to simulate the fibers. The interaction of the fibers was able to mimic by employing the discrete element method. The fiber distribution was captured and compared to the experiment. The simulation results were able to reveal the fiber deposition layer upon layer and explain the formation of uneven thickness in the tilted area of the molded fiber screen.

Keywords: 3D printing, molded fiber screen, multi-sphere model, discrete element method.

1. INTRODUCTION

In the past several decades, plastic-based products have been widely used in the packaging industry due to their high performance, low cost, light weight, and easy processing

[1]. However, most of the plastic products are non-biodegradable, causing plastic pollution, which threatens even human health [2]. It is an alarm for scientists and human beings to find an alternative solution to replace plastic-based packaging products. In recent years, molded fiber products have attracted attention due to their renewability, recyclability, sustainability, and biodegradability [3]. Hence, molded fiber products become a strong candidate to reduce the plastic waste from the packaging industry.

In conventional manufacturing, meshing tools were employed to fabricate molded fiber products [4]. However, it faces the limitation in fabricating complex geometry. It is known that pore size, shape, tilted angle of the pore axis, pore arrangement, and surface structure directly affect the de-watering speed of the molded fiber screen. However, it is challenging to arrange the meshing tools to generate these changes in the pore size, shape, and tilted angle of the pore axis by the conventional method. Hence, in recent years, 3D printing has been adopted to fabricate molded fiber screen [5]. It allows the fabrication of complex geometries, suitable for complex packaging. In addition, the pore size and shape can be varied without any hindrance [6].

The 3D printing molded fiber screen is still in progress to design the novelty screen to enhance the de-watering speed, fiber collection, and increase its strength. In fact, the molded fiber products experience the unevenness of their thickness at different locations, especially at the tilted surface. There is a need to understand the cause of this issue, and it can be revealed by capturing the fiber deposition on the screen.

Some propose using an experimental setup to capture the fiber deposition on the screen. However, due to the condensation of fiber inside the slurry, it brings great challenges to assess the fiber depositing on the screen. Hence, the modelling technique is a useful tool to capture the fiber deposition on the screen.

In the prior study, Lagomarsino, Pagonabarraga, and Lowe simulated an elastic filament in the fluid on a microscopic scale where the bending of the filament depended on the applied forces [7]. In addition, Delmotte, Climent, and Plouraboué employed the bead model to simulate a flexible fiber at low Reynolds number [8]. The model provided a flexible framework without adding artificial forces, and it is suitable for the simulation of micro-organisms, membranes, and micro-mechanics. Besides, Hosseini and Tafreshi solved a computational fluid dynamics (CFD) code with the discrete element method (DEM) to simulate the fiber collected on the filtration surface [9]. Moreover, Wang, Zhao, Wang, He,

and Zheng employed the Lattice-Boltzmann method to simulate the two-phase model for the filtration process [10].

In this study, the multi-sphere model was employed to simulate the pulp fiber made from wood. Using a multi-sphere model allows for generating fibers in different geometries and different orientations to mimic the experiment as closely as possible. This study aims to adopt the simulation results to reveal the defects obtained in the experiment.

2. METHODOLOGY

In the DEM model, each fiber was simulated as a clump of particles. The particle within the same clump has no interaction; however, the interaction of particles belonging to different clumps was considered. The displacement and rotation of each clump were calculated based on the following equations [11]:

$$m_i \frac{d\boldsymbol{U}_i}{dt} = m_i \boldsymbol{g} + \sum_j \boldsymbol{F}_{i,j} + \boldsymbol{F}_{i,f}, \quad (1)$$

$$\boldsymbol{I}_i \frac{d\boldsymbol{\omega}_i}{dt} + \boldsymbol{\omega}_i \times (\boldsymbol{I}_i \cdot \omega_i) = \sum_j \boldsymbol{M}_{i,j} + \boldsymbol{M}_{i,f}, \quad (2)$$

where m_i is the mass of the clump *i*, U_i is the velocity of the clump *i,* **g** is gravitational acceleration, $F_{i,j}$ is the inter-particle contact force between sub-particles in clump *i* and *j*, and $F_{i,f}$ is the fluid force on clump *i*. $\boldsymbol{I}_i$ is the inertia tensor of clump *i*, $\boldsymbol{\omega}_i$ is the rotation velocity of clump *i*, $\boldsymbol{M}_{i,j}$ is the moment due to particle-particle interaction of those belong to clump *j* interacting on clump *i*, and $\boldsymbol{M}_{i,f}$ is the moment of clump *i* due to the fluid force. In this simulation, a natural drying process due to the gravity force was considered, and the fluid force was not considered in the simulation result.

The fibers were simulated in three different orientation including horizontal, vertical, and titled angle to represent the fiber mixture inside the slurry as depicted in Figure 1.

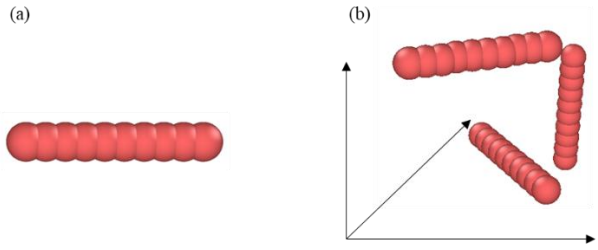

Figure 1. The morphology of (a) single fiber and (b) initial fiber orientation in the model

The simulation domain $x \times y \times z = 10 \times 10 \times 22$ mm^3 as shown in Figure 2. The simulated domain is sufficient to represent the 3D molded fiber screen where the local area of the actual screen morphologies was fully captured. The same volume of fiber was set in the simulation. The material properties used in the simulation are listed in Table 1.

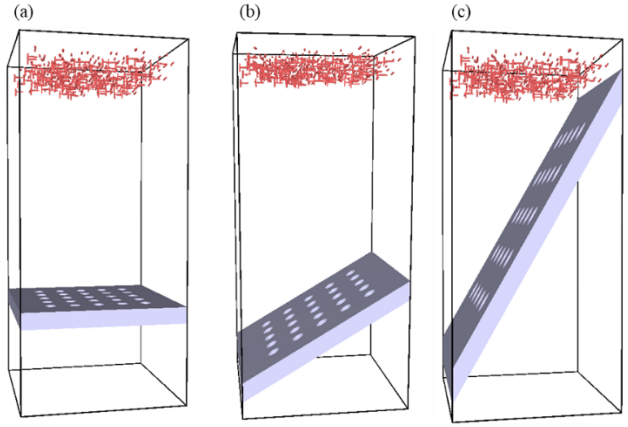

Figure 2. Same volume of fibers inserted in the domain to deposit on (a) flat screen, (b) 30°-tilted screen, and (b) 60°-tilted screen

In addition, an experiment was also performed to validate the simulation result. The experimental setup consisted of MJF 3D printed screens, a slurry solution, and a natural drying process. The MJF 3D printed screens were printed by HP Jet Fusion 5200 using polyamide-11 (PA11). The stereolithography (STL) files were designed in the same way as the ones used in the DEM model. The slurry solution consists of 0.5% wood fibers blended with water, and then 350 mL of slurry was poured on top of the screen, and due to the gravity, the fibers were collected on top of the screen. Followingly, these molded fiber samples were dried in the oven at a temperature of 80°C for 1 hour to fully dry the samples. The dried samples were used to validate the simulation results.

Table 1. Material properties using in the DEM model

Material properties	Value	Unit	Reference
Density of wet wood	1500	kg/m^3	[12]
Youngs Modulus	0.01	GPa	[13]
Poisson Ratio	0.25	-	[14]
Coefficient Restitution	0.15	-	[15]
Coefficient Friction	0.11	-	[13]

3. SIMULATION RESULTS

Figure 3 shows the fibers deposited on screens. As observed at 40 ms, the fibers started to touch the 60°-tilted screen and rolled on the screen, while the same fibers had not yet reached the flat screen or the 30°-tilted screen. In addition, when the fibers had settled down, the fiber deposition on the flat screen and on the 30°-tilted screen was more even as compared to that on the 60°-tilted screen. By employing the 60º-tilted screen, the fibers tended to slide to the lower area of the screen. This is due to the gravity force pulling the fibers to slide downward, leading to a large area of the screen in the upper area that was unable to capture the fibers, as shown in Figure 3(*c*)(*iv*).

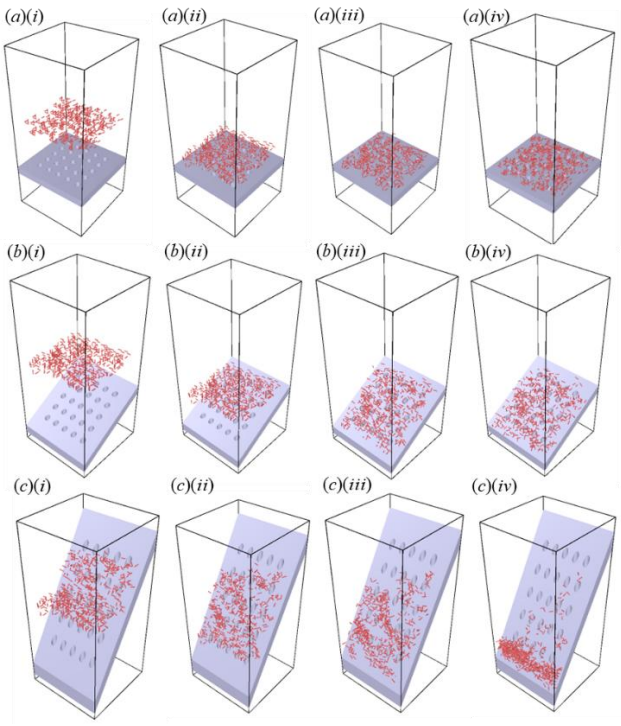

Figure 3. Fiber deposition on (a) flat screen, (b) 30°-tilted screen, and (b) 60°-tilted screen at (*i*) t = 40 ms, (*ii*) t = 50 ms, (*iii*) t = 60 ms, and (*iv*) t = 100 ms.

In addition, the experiment was performed to validate the simulation result. It shows that for the flat screen and the 30°-tilted screen, the fibers were distributed and covered the whole screen area. However, for a 60º-tilted screen, a large area of the screen surface was not able to capture the fibers, and most of the fibers sank to the bottom area of the screen. Hence, it formed a large area where fibers were unable to cover. It explains the phenomena obtained in the simulation as shown in Figure 3, where the flat screen and the 30°-tilted screen were well covered by the fibers, while the 60°-tilted screen left a large area with no fibers

remaining on the surface of the screen. Although there was a gap between the experiment and the simulation result. Firstly, it can be explained that the number of fibers in the experiment is hundreds of times larger than that in the simulation. Secondly, the DEM model was set up without the effect of surface tension and viscous force. However, the simulation results were obtained that reflect the ones in the experiment. Therefore, the simulation model can be used to reveal the phenomena in the experiment.

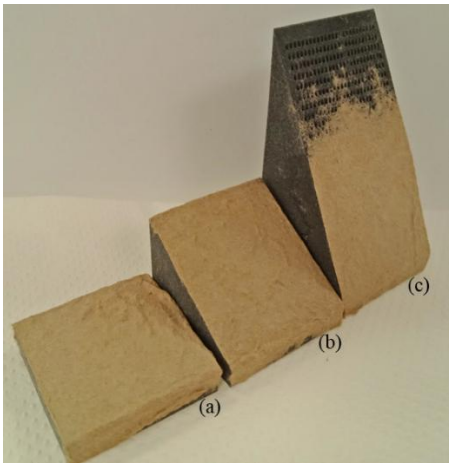

Figure 4. Experimental fiber deposition on (a) flat screen, (b) 30°-tilted screen, and (b) 60°-tilted screen

4. CONCLUSIONS

The study investigated the fiber deposition on different molded fiber screens by simulation and experiment. It found that the tilted screen with a high tilted angle, such as 60°, containing a large area of the screen surface, was unable to collect the fibers. It was because most of the fibers sank to the bottom of the screen. Hence, it explained the defect of uneven thickness of the highly tilted surface of the molded fiber product.

ACKNOWLEDGEMENT

This study was supported under the RIE2020 Industry Alignment Fund – Industry Collaboration Projects (IAF-ICP) Funding Initiative, as well as cash and in-kind contribution from the industry partner, HP Inc. This research was continued to be supported by VNU Vietnam Japan University under the project VJU.GV.25.02.

DISCLOSURE STATEMENT

Nothing to declare.

REFERENCES

[1]. Schneiderman, D. K., and Hillmyer, M. A. (2017). There is a great future in sustainable polymers, *Macromolecules*, vol. 50(10), p. 3733-3749.

[2]. Horejs, C. (2020). Solutions to plastic pollution, *Nature Reviews Materials*, vol. 5(9), p. 641-641.

[3]. Didone, M., and Tosello, G. (2019). Moulded pulp products manufacturing with thermoforming, *Packaging Technology and Science*, vol. 32(1), p. 7-22.

[4]. Keyes, F. E. (1890). Method of molding pulp articles, *Patent No*. US424003A.

[5]. Saxena, P., Bissacco, G., Meinert, K. Æ., Danielak, A. H., Ribó, M. M., and Pedersen, D. B. (2020). Soft tooling process chain for the manufacturing of micro-functional features on molds used for molding of paper bottles, *Journal of Manufacturing Processes*, vol. 54, p. 129-137.

[6]. Andersson, J, Vogt, U., and Pierce, D. A. (2010). Tool or tool part, system including such a tool or tool part, method of producing such a tool or tool part and method of molding a product from a pulp slurry, *Patent No*. US20170370049A1.

[7]. Lagomarsino, M. C., Pagonabarraga, I., and Lowe, C. P. (2005). Hydrodynamic induced deformation and orientation of a microscopic elastic filament, *Physical review letters*, vol. 94(14), p. 148104.

[8]. Delmotte, B., Climent, E., and Plouraboué, F. (2015). A general formulation of Bead Models applied to flexible fibers and active filaments at low Reynolds number, *Journal of Computational Physics*, vol. 286, p. 14-37.

[9]. Hosseini, S. A., and Tafreshi, H. V. (2012). Modeling particle-loaded single fiber efficiency and fiber drag using ANSYS–Fluent CFD code, *Computers & Fluids*, vol. 66, p. 157-166.

[10]. Wang, H., Zhao, H., Wang, K., He, Y., and Zheng, C. (2013). Simulation of filtration process for multi-fiber filter using the Lattice-Boltzmann two-phase flow model, *Journal of Aerosol Science*, vol. 66, p. 164-178.

[11]. Shen, Z., Wang, G., Huang, D., and Jin, F. (2022). A resolved CFD-DEM coupling model for modeling two-phase fluids interaction with irregularly shaped particles, *Journal of Computational Physics*, vol. 448, p. 110695.

[12]. Kellogg, R. M., and Wangaard, F. F. (1969). Variation in the cell-wall density of wood, *Wood and Fiber Science*, no. 3, p. 180-204.

[13]. Guo, Y., Chen, Q., Xia, Y., Westover, T., Eksioglu, S., and Roni, M. (2020). Discrete element modeling of switchgrass particles under compression and rotational shear, *Biomass and Bioenergy*, vol. 141, p. 105649.

[14]. Sheng, Y., Wang, M., Zhang, L., and Ren, Q. (2022). Analysis of filtration process of 3-D mesh spacer filter by using CFD-DEM simulation, *Powder Technology*, vol. 396, Part B, p. 785-793.

[15]. Qian, F., Huang, N., Zhu, X., and Lu, J. (2013). Numerical study of the gas–solid flow characteristic of fibrous media based on SEM using CFD–DEM, *Powder technology*, vol. 249, p. 63-70.